LIMNOLOGY and OCEANOGRAPHY

ASLO

Limnol. Oceanogr. 68, 2023, 1865–1879

doi: 10.1002/lno.12391

Combining modeling with novel field observations yields new insights into wintertime food limitation of larval fish

Anna Akimova,[1*] **Myron A. Peck**,[2] **Gregor Börner**,[3] **Cindy van Damme**,[4] **Marta Moyano**[5,6]

[1]Thünen-Institute of Sea Fisheries, Bremerhaven, Germany
[2]Department of Coastal Systems, Royal Netherlands Institute for Sea Research, Texel, The Netherlands
[3]Institute of Marine Ecosystem and Fishery Science, Hamburg University, Hamburg, Germany
[4]Wageningen Marine Research, IJmuiden, The Netherlands
[5]Norwegian Institute for Water Research (NIVA), Oslo, Norway
[6]Center for Coastal Research, University of Agder, Kristiansand, Norway

Abstract

Recruitment success of marine fishes is generally considered to be highly dependent on larval growth and survival. In temperate ecosystems, fish larvae are sensitive to food limitation during the low productivity seasons, particularly if water temperatures and concomitant larval metabolic costs increase due to climate change. We combined 7 years of in situ sampling of larval fish, novel observations on zooplankton via automated image analyses, and larval physiological modeling to explore feeding conditions of Atlantic herring larvae (*Clupea harengus*) in the North Sea. The observed plankton size-structure was close to the theoretical optimum for larval foraging, but not the biomass. Our results for autumn larvae supported Hjort's critical period hypothesis: small first-feeding larvae were predicted to have a high probability of starvation, whereas larvae > 13 mm were able to reach their maximal growth capacity. In winter, the majority of herring larvae of all tested sizes (5–27 cm) experienced food-limitation with over 35% probability of starvation. Sensitivity analysis suggested that young herring larvae improve their growth performance and probability of survival if feed not only on copepods and their life-stages but include other microplankters in their diet. Given projected warming of the North Sea, our model predicts that herring larvae would require 28% (35%) more prey biomass in autumn (winter) to sustain their growth and survival in the future. This finding together with the ongoing low recruitment of North Sea herring underscore the importance of future micro- and mesoplankton monitoring within a scope of wintertime larval fish surveys.

Fish early life is widely acknowledged as a critical period determining variation in fish recruitment and, to a large extent, the population size of various fish species (e.g., Chambers and Trippel 1997; Fuiman and Werner 2002). The larval stage is often considered as the main bottleneck due to high starvation and predation mortality (Bailey and Houde 1989; Pepin et al. 2015). Several prominent recruitment hypotheses linking larval foraging success, growth and survival have emerged in the of 20th century, starting with the "critical period" hypothesis of Hjort (1914) and moving towards more complex concepts of "growth-survival," "stage duration," and "bigger is better" (e.g., Anderson 1988; Houde 2008). Temporal match between fish larvae and the spring "bloom" of their planktonic prey is considered a key factor determining larval survival and recruitment in spring spawning fish species (Cushing 1990; Peck et al. 2012). Less is known about tropical fishes spawning in oligotrophic waters (Llopiz 2013) and temperate fishes spawning in a low-productivity period, such as autumn or winter. Larvae from the latter group encounter lower temperatures as well as shorter photoperiods as they develop. Prey abundance and composition are often poorly studied in this low-productivity season and larval dietary preferences are less known (Robert et al. 2014). All this can potentially lead to biased estimates of the food-limited larval growth as well as starvation mortality. A better mechanistic understating of larval foraging success in winter spawning fishes is requited to assess and project the

*Correspondence: anna.akimova@thuenen.de

Additional Supporting Information may be found in the online version of this article.

Author Contribution Statement: A.A., M.M. and M.A.P. conceived the study. A.A. performed data analyses, numerical simulations and their interpretation, and drafted the article. M.M. and M.A.P. substantially contributed to the critical revision of the article. G.B. and C.v.D. collected and processed field samples. All authors discussed the results and approved the final version of the article. M.M. supervised the project.

consequences of climate-driven variability and shifts in direct (e.g., temperature) and indirect (prey abundance and type) factors affecting their recruitment.

North-Sea autumn spawning herring (NSASH), one of the most commercially important pelagic stocks, is known to spawn between August and January in four main areas in the North Sea: Orkney-Shetland, Buchan, Banks, and Downs (Dickey-Collas et al. 2010; Fig. 1a). NSASH has a long history of exploitation, including a stock collapse caused by recruitment overfishing and subsequent recovery (Fig. 1b; Geffen 2009; Payne et al. 2009; Dickey-Collas et al. 2010). Since 2002, this stock has experienced a sustained period of low recruitment that has alarmed fisheries scientists and managers. Previous studies showed that the poor recruitment success is mainly caused by elevated rates of larval mortality (e.g., Nash and Dickey-Collas 2005; van Damme et al. 2009; Illing et al. 2018), but possible mechanisms are still debated. Starvation has been often suggested as the main mortality source of herring larvae (Payne et al. 2013; Alvarez-Fernandez et al. 2015; Hufnagl et al. 2015), but the lack of field observations of prey abundance, size-structure and species composition during autumn and winter in the North Sea was identified as one of the major gaps in our understanding of larval growth and survival.

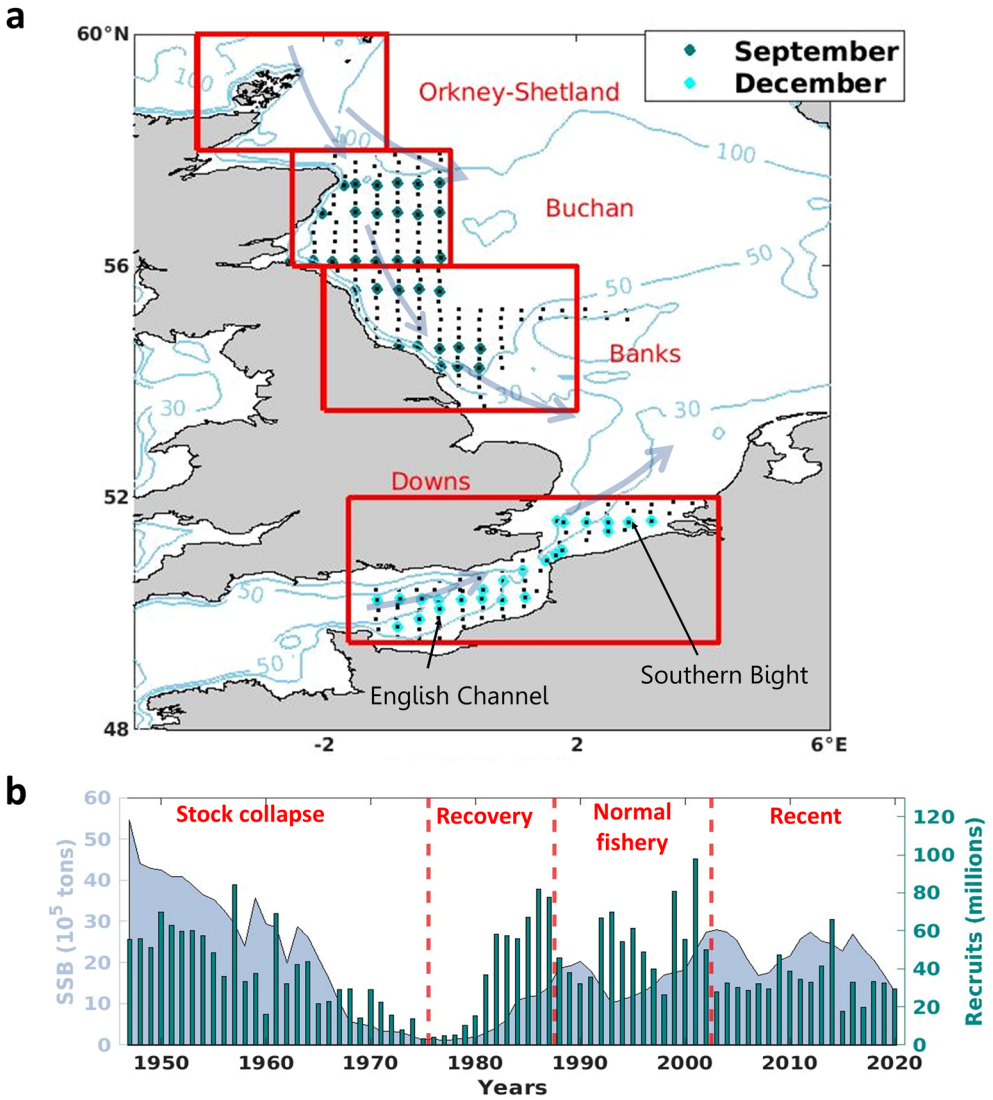

Fig. 1. (**a**) Study region in the western North Sea. Plankton samples taken in September (teal) and December (cyan) are shown together with a typical sampling grid of the Netherland's contribution to the International Herring Larvae Survey (black dots), where herring larvae were sampled. Known spawning locations (Orkney-Shetland, Buchan, Banks and Downs) of the North Sea Autumn Spawning Herring stock (NSASH) are identified. Black arrows show two subareas in the Downs spawning area (English Channel and Southern Bight). Light-gray arrows show the direction of prevailing currents. (**b**) Annual changes in spawning stock biomass (SSB, gray area) and the number of recruits (teal bars) of NSASH as obtained from the ICES stock assessment (https://www.ices.dk/data/assessment-tools/Pages/stock-assessment-graphs.aspx, accessed on 1 June 2022). Red dashed lines identify phases of herring stock history after Payne et al. (2009).

The main objective of our study was to investigate the feeding conditions that young herring larvae experience during their first month of life in the North Sea and whether these conditions differ among autumn- and winter-spawning sites. To describe the available prey, we used size- and taxa-resolved information on micro- and mesoplankton collected simultaneously with herring larvae. A physiological model simulating larval foraging and growth used the observed prey fields to test the hypothesis that recent, poor recruitment of North Sea herring was linked to suboptimal feeding conditions of its larvae and that the available prey was largely insufficient to cover larval energy requirements. We tested two feeding scenarios to assess whether a broader generalist feeding strategy of larvae is beneficial in comparison to a specialist (only copepods) feeding mode in the low-productivity season. Furthermore, given a projected rise of water temperatures in the North Sea by the end of the 21st century (on average 2.0°C, Schrum et al. 2016), we estimated how the zooplankton biomass and/or size composition would need to change to meet the increasing energy demand of herring larvae in the future climate.

Data and methods

Data

Zoo- and phytoplankton, larval abundance and water temperature data were collected during the International Herring Larvae Survey (IHLS) in the North Sea between 2013 and 2019. In this study, we considered a merged Buchan and Banks area (further on Buchan/Banks) east of the British Isles, where herring is known to spawn in September, and the Downs area in the English Channel and Southern Bight, where spawning occurs in December–January (Fig. 1a). Herring larvae and mesozooplankton were sampled using a Gulf VII high-speed sampler (280 μm mesh size, 0.2 m nose cone opening; Nash et al. 1998) and conducting double-oblique hauls from the surface to 5 m above the bottom. A PUP-net (55 μm mesh size) was attached to the Gulf VII and sampled microplankton. In total, between 27 and 35 (14 and 25) zooplankton samples were collected yearly in the Buchan/Banks (Downs) area depending on weather conditions (Table S1 in the supplements). A sample analysis is described in the supplementary materials (S1 "Plankton data"). In this study, we included 11 taxonomic groups: copepods, appendicularians, bivalve larvae, gastropod larvae, echinoderm larvae, ciliates, cladocerans, diatoms, dinoflagellates, foraminiferans, and silicoflagellates. These planktonic organisms were considered suitable for larval feeding based on their size, geometric form and previous studies identifying them as larval prey (Last 1978; Pepin and Penney 1997; Robert et al. 2014).

Captured herring larvae were preserved in formalin, total length of each larva was measured with the accuracy of 1 mm and abundance-at-length was assessed. Developmental stages of herring larvae (yolk-sac, pre-flexion, flexion, and post-flexion) per size class were documented. We refer the reader to Schmidt et al. (2009) for further technical and methodological details on larval sampling. Data on water temperature were collected using a Seabird CTD (conductivity, temperature, depth) SBE 911 profiler mounted on the Gulf VII sampler. We calculated the mean temperature along the entire water column at each station to match depth-integrated plankton and larval samples.

Methods

Observed prey fields and larval length-at-first-feeding

To provide the prey field for the larval foraging model, we calculated a zooplankton normalized biomass size spectra (NBSS) based on the empirical paradigm of Sheldon's spectra (Sheldon et al. 1972; Blanco et al. 1994). We first converted the equivalent spherical diameter (ESD_z, in μm, S1 "Plankton data") measured for each zooplankton organism to its individual dry weight w_z (in μg) using the equation of Huebert et al. (2018) (their Eq. A3), adapted to μm instead of mm originally used:

$$w_z = 4.43 \cdot 10^{-7} \cdot ESD_z{}^{2.5} \quad (1)$$

Based on their dry weight w_z, planktonic organisms were grouped in size bins on the octave scale and the bin-specific biomass was calculated by summing all individual weights within each size bin. To obtain the normalized size spectrum β_z, we divided the bin-specific biomass by the width of the corresponding weight intervals Δw_z. We calculated β_z at each station and fitted a weighted linear regression to β_z on the log–log scale with the regression weights being proportional to the observed zooplankton abundances within each size bin. Undersampled size-bins, that is, size-bins with the observed abundances below 0.01% of the total abundance or located to the left of the modal size-bin of PUP and Gulf VII samples, were excluded (Álvarez et al. 2013). The normalized biomass spectrum β_z was then used to calculate the zooplankton biomass B_z:

$$B_z = \int \beta_z \cdot dw_z = \int a \cdot w_z{}^s \cdot dw_z = \begin{cases} a \cdot \ln w_z, \text{if } s = 1 \\ a \cdot w_z{}^{s+1}, \text{if } s \neq 1 \end{cases} \quad (2)$$

where dw_z is the differential of w_z, s is the slope and a is the intercept of the linear regression fitted to β_z on the log–log scale. Following previous modeling studies of Hufnagl and Peck (2011) and Huebert and Peck (2014), we used zooplankton in the size range between 20 and 2000 μm as a prey field for the modeled larvae.

Length measurements and staging performed on captured herring larvae were used to obtain a field-based estimate of the larval length-at-first-feeding (LFF). Wild caught herring larvae rapidly lose their yolk-sac; therefore, it was not feasible to estimate the minimal LFF from the captured larvae and we only estimated the maximal size of yolk-sac larvae as a proxy to the maximal LFF. The measured length of the formalin preserved larvae was converted to the length of fresh larvae (*see* S2 "Bias correction of larval length due to formalin preservation"). This resulted in a range in larval sizes between 5.3 and

26.2 mm. We split the Downs observations into two subareas (the English Channel and the Southern Bight areas; Fig. 1a) and built the mean size-frequency distributions for yolk-sack and no-yolk-sac larvae for the Buchan/Banks and each subarea within Downs over the observed period 2013–2019.

Bioenergetic model

The individual-based bioenergetic model of herring larvae was mainly based on Hufnagl and Peck (2011) with some modifications described in the supplementary materials (S3 "Model description"). Our model kept energy housekeeping of an individual herring larva in form of a growth equation:

$$G = E_{gain} - E_{loss} = C \cdot AE - (C \cdot AE \cdot \mathrm{SDA} + k \cdot R_s) \quad (3)$$

where G is energy available for somatic growth, E_{gain} is the energy C gained from foraging weighted by the assimilation efficiency AE, E_{loss} is the energy spent for the metabolic costs such as specific dynamic action SDA and the standard respiration rate R_s. An activity multiplier k was $k = 2.5$ during the day and $k = 1$ during the night following Huebert and Peck (2014). Since herring larvae are visual predators, their active feeding was limited to the photoperiod (length of daylight): 12 h in September and 8 h in December, respectively. The energy income C was modeled based on the optimal foraging approach that mechanistically simulates larval selective feeding based on the relative sizes of a herring larva and its prey (Letcher et al. 1996). This approach allowed us to study the variability in larval growth linked to the prey abundance and size structure, as well as the length of the photoperiod. Metabolic costs R_s and AE were temperature- and size-dependent and allowed to study the influence of temperature on the growth rate of herring larvae of various initial size. The detailed description of the model equations is provided in the supplementary materials (S3 "Model description").

In each simulation, we initiated one larva per 0.1-mm size intervals between 5 and 27 mm to cover the observed range in larval size and simulated 1 day of life of each larva. The larvae of all size-classes were initiated at each station regardless whether such larvae were observed at this station or not. The reason for this was that the observed larval abundance is already the outcome (survivors) of mortality rates being experienced by larval cohorts in the field, including starvation mortality, which we aimed to assess in our study. We estimated the daily specific growth rate (SGR, in percent dry weight per day, further on % dw d^{-1}) from 24-h (1 day and one night) simulations as:

$$SGR = 100 \cdot (w_{l1} - w_{l0}) \cdot 1/w_{l0} \quad (4)$$

where w_{l0} and w_{l1} were larval weights at the beginning and at the end of the simulation, respectively. In each simulation and for each initial larval length, we estimated the ad-libitum larval growth or the maximal growth capacity (SGR_{max}) by gradually increasing prey concentration until the modeled growth rate reached its maximum and stagnated. Herring larvae were considered to experience starvation if the predicted SGR was ≤ 0, food-limited growth if $SGR > 0$ and $SGR < SGR_{max}$ and prey satiation, that is, ad-libitum growth, if $SGR = SGR_{max}$.

Model simulations

We conducted three groups of model simulations: (1) diet preference scenarios, (2) growth predictions using in situ prey fields, and (3) optimal and future feeding conditions. In the "diet preference" simulations, we tested two scenarios of larval feeding: (1) "specialist," where only copepods were included as a suitable prey, and (2) "generalist," where 11 taxonomic groups of plankton were considered as potential prey. For both scenarios, we used the average NBSS obtained with corresponding zooplankton organisms and the area-specific median temperatures: 12.3°C for Buchan/Banks and 10.9°C for Downs.

To predict larval growth at in situ prey fields, we simulated daily SGR of herring larvae at each station using the station-specific water temperature, zooplankton NBSS slope and biomass that corresponded to the generalist feeding scenario. The simulated growth rate was expressed as a proportion of SGR_{max} in order to isolate the effects of prey limitation from the temperature- and size- dependency in larval growth. To clearly demonstrate the differences between spawning seasons/areas, we pooled predicted growth rates for all stations within each season and calculated the proportion of stations where the modeled larvae were predicted to grow at a certain growth rate.

In the simulations of the "optimal and future feeding conditions," we first set water temperature to its area-specific median values and estimated larval growth at a wider range of the zooplankton concentrations between 0.1 and 1000 mg m^{-3} and a range of the NBSS slope between −1.7 and −0.1, covering the observed and previously reported variability of the zooplankton size-spectrum slope in the North Sea (Hufnagl and Peck 2011; Huebert et al. 2018). For each larval length, we identified two values: (1) the minimal prey biomass required for a positive larval growth (starvation point, B_{min}), and (2) an optimal NBSS slope that corresponds to the B_{min}. We further investigated how B_{min} varies with temperature between 8°C and 17°C, that is, within the range of the observed and future (projected) temperatures in the North Sea in autumn and winter. The optimal NBSS slope did not depend on temperature or season, because neither temperature nor light conditions were included in the formulation of the larval size-based prey selectivity (*see* S3 "Model description").

Results

Observed plankton and herring larvae

The total plankton biomass B_z of all 11 taxonomic groups in the range of sizes between 20 and 2000 μm was, on average, 3 times lower in winter in Downs (median of 3.4 mg m^{-3} Fig. 2f) than in autumn in Buchan/Banks areas (median of 9.4 mg m^{-3}). The mean NBSS slope was significantly (*t*-test, $t[280] = 9.64$,

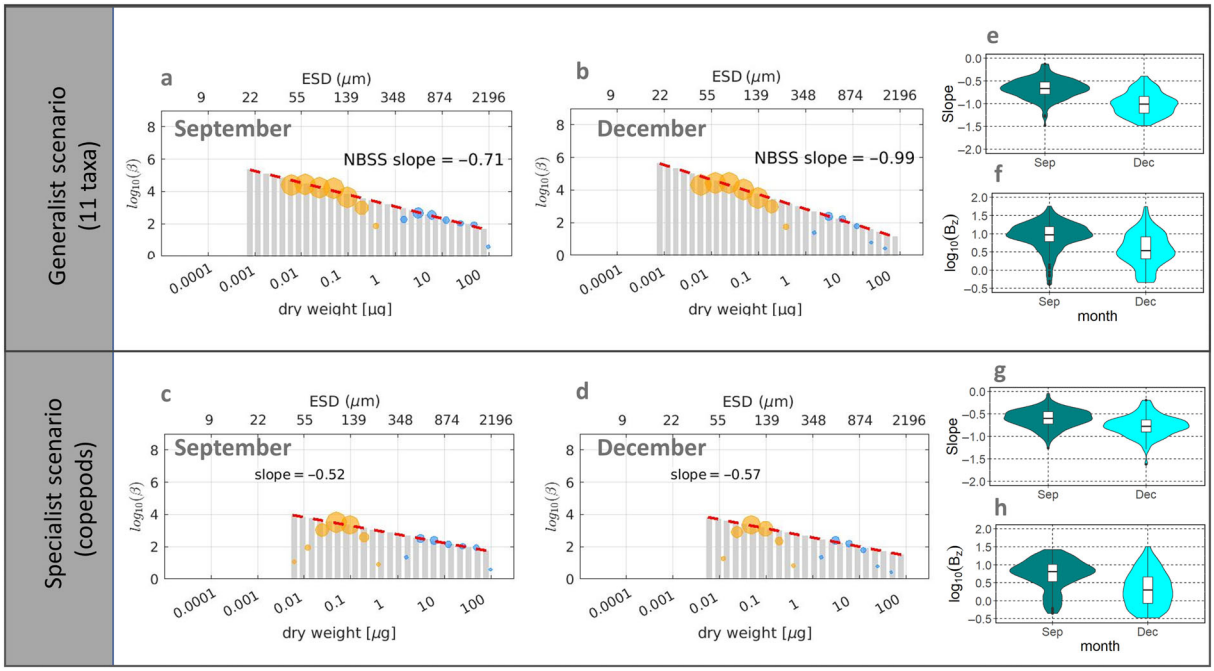

Fig. 2. Mean normalized biomass size spectra (NBSS, β_z) obtained with 11 prey taxa (**a**—September, **b**—December), and with only copepods (**c**—September, **d**—December). Circles display the mean observed normalized biomass averaged over all stations within the season/spawning area measured with a Flowcam (orange) and Zooscan (blue). The size of the circles is proportional to the log-abundance of the zooplankton organisms in corresponding size-bins. Under-sampled size-classes were excluded (see text). Red dashed lines show the weighted linear regression fitted to the observed NBSS. Gray bars indicate the zooplankton size-classes used in the "generalist" and "specialist" feeding model scenarios. ESD stays for the equivalent spherical diameter. The distributions of the observed NBSS slope and the total zooplankton biomass with 11 prey taxa (**e** and **f**) and with only copepods (**g** and **h**) are shown for both seasons/spawning sites (teal—September [Buchan&Banks], cyan—December [Downs]). The zooplankton biomass B_z in **f** and **h** is in mg m^{-3}.

$p<0.01$) steeper in December (−0.99; Fig. 2b) than in September (−0.71; Fig. 2a). Copepods were the most abundant taxa (between 73% and 100% of the biomass) of the mesozooplankton but their proportion decreased toward the low end of the size-spectra (i.e., $ESD<200\,\mu$m). No copepods with *ESD* smaller than 40 μm were observed (Figs. 2c,d and S4), therefore, all size-classes smaller than 40 μm were excluded from the size-spectra used in the "specialist" feeding scenario simulations (Fig. 2c,d, gray bars).

Larval length-frequency distributions as well as the proportion of the yolk-sac larvae differed among the spawning areas (Fig. 3). In the Buchan/Banks area, herring larvae up to 26 mm were observed and the largest yolk-sac larvae were recorded in the size-class between 9.7 and 10.8 mm (Fig. 3a). As for the Downs area, a larger proportion of smaller larvae was observed in the English Channel in comparison to the Southern Bight (Fig. 3b,c). The largest yolk-sac larvae were reported in the size class between 11.9 and 13.0 mm in both subareas.

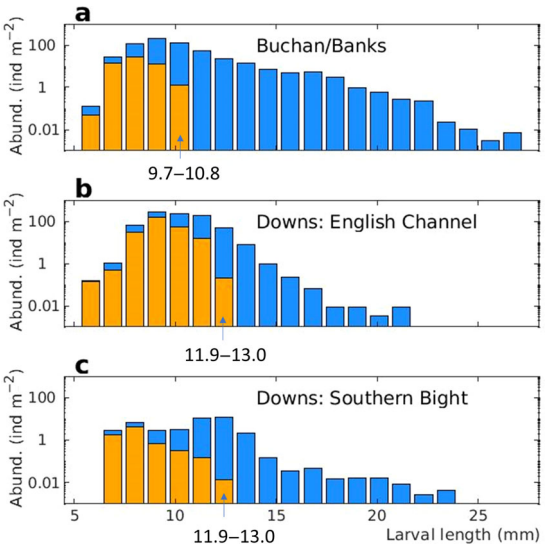

Fig. 3. The mean length-frequency distributions of yolk-sac (orange) and post-yolk (blue) herring larvae observed in the Buchan/Banks areas in September (**a**), in the English Channel (**b**) and the Southern Bight (**c**) in December. Larval length was corrected accounting for the shrinkage occurring during preservation. Larval abundances were averaged over the 2013–2019 period. Arrows indicate the largest size-classes of the observed yolk-sac larvae and the corresponding size-range is annotated.

Simulation 1 "diet preference": Model sensitivity to the choice of the larval feeding scenario

Larval growth rates obtained in the specialist and generalist scenarios varied with larval length and differed between the spawning seasons/areas (Fig. 4). In the specialist scenario (blue

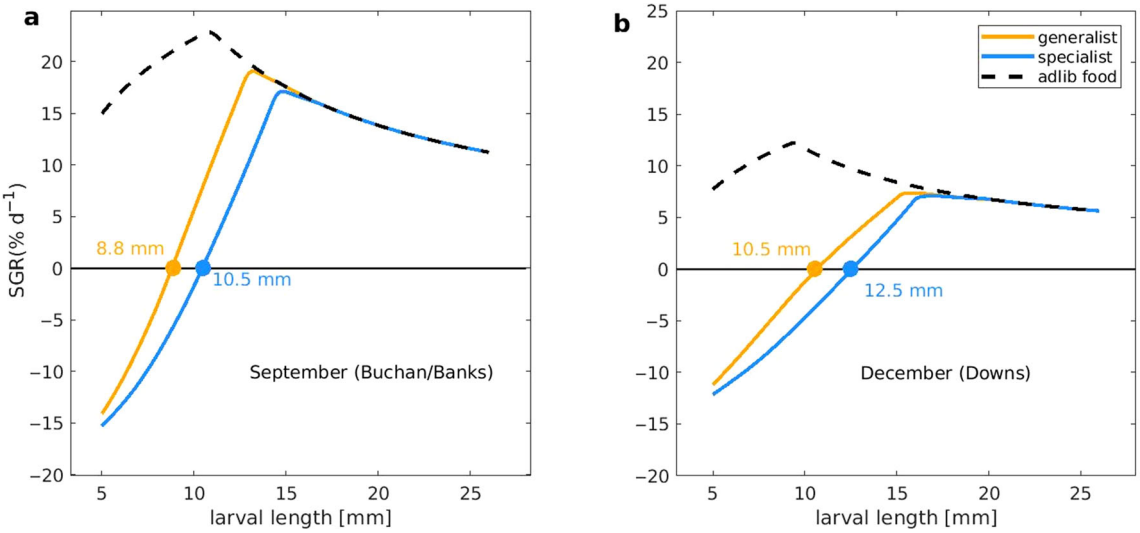

Fig. 4. Simulated larval specific growth rate (*SGR* in % dw d^{-1}), obtained in the generalist (orange) and specialist (blue) feeding scenarios with the mean normalized biomass size-spectra in September (**a**) and December (**b**). Black dashed curves show the modeled "ad-libitum" growth at the corresponding environmental conditions (Buchan/Banks areas – $T = 12.3°C$, photoperiod = 12 h; Downs – $T = 10.9°C$, photoperiod = 8 h). Black solid lines identify zero-growth. Orange and blue circles indicate minimal larval length, at which modeled larvae were able to sustain a positive growth in corresponding feeding scenarios.

curves in Fig. 4), herring larvae smaller than 10.5 (12.5) mm in September (December) were not able to sustain their growth (predicted growth rates were negative). In the generalist scenario (orange curves in Fig. 4), our model predicted a positive growth for smaller larvae in comparison to the specialist scenario in both spawning seasons (8.8 mm in September and 10.5 mm in December).

The maximal-growth capacity SGR_{max} (black dashed curves in Fig. 4) changed with larvae size in a similar way in both seasons, but was reduced by almost half in December (between 7% and 13% dw d^{-1}, Fig. 4b) compared to September (between 12% and 25% dw d^{-1}, Fig. 4a) due to a combined effect of a lower temperature and a shorter photoperiod. Independently of the season, the growth rate predicted in the specialist scenario was about 40% that in the generalist scenario. At the mean prey concentrations tested, herring larvae were predicted to be food-limited in both feeding scenarios until they reached the length of 16.3 and 20.5 mm in September and December correspondingly.

The role of the microzooplankton in larval foraging was assessed from the generalist feeding scenario. The foraging niche was found to broaden with increasing larval size and to narrow when the food availability increased. At two tested prey concentrations (0.3 and 6.3 mg m^{-3}), which correspond to the 2.5th- and 50th-percentiles of the observed biomass in both seasons, larvae of all size-classes were predicted to include microplankton prey in their diet (Fig. 5). The proportion of microplankton in the larval diet decreased with the larval size and constituted, for example, 38% and 4% for an 8-mm and a 23-mm larva, correspondingly. Only at the highest observed zooplankton biomass (90.9 mg m^{-3}), larger larvae (> 18 mm) were predicted to exclude microplankton from their diet.

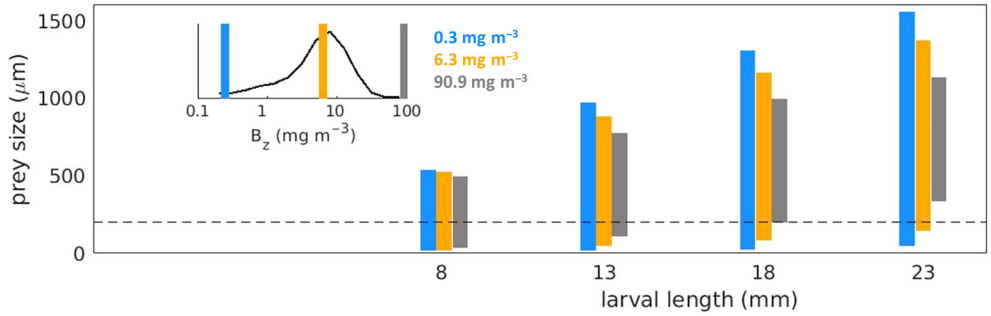

Fig. 5. The width of the foraging niche of an 8-, 13-, 18-, and 23-mm herring larva obtained in the simulations with the minimal (0.3 mg m^{-3}; blue), median (6.3 mg m^{-3}; orange) and maximal (90.9 mg m^{-3}; gray) observed prey biomass and a constant NBSS slope of −0.77, which was the median of all observed slopes. The black dashed line indicates 200 μm as a separation between micro- and meso- plankton. The inlet shows the frequency distribution of the observed zooplankton biomass (B_z) and the color bars show the corresponding prey biomasses used to calculate the foraging niches.

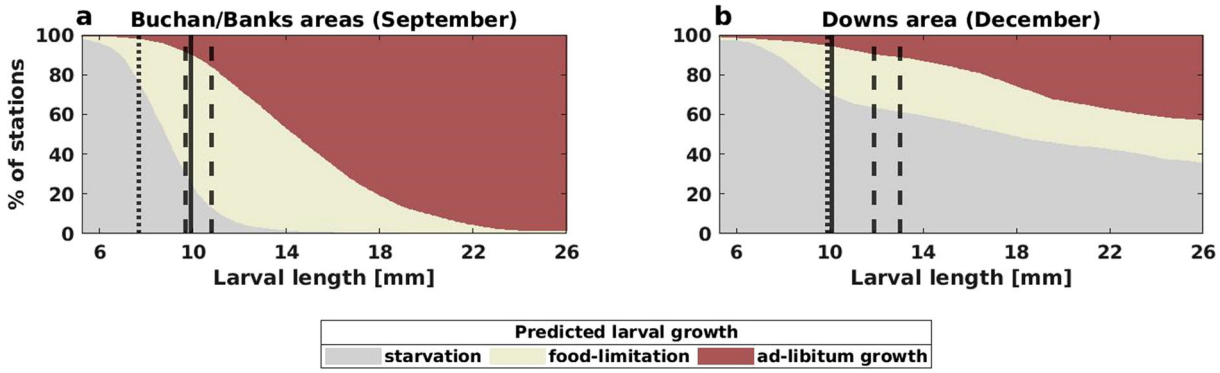

Fig. 6. The fraction of stations (in %) where the modeled larvae of different length were predicted to experience starvation ($SGR \leq 0$, gray), food-limitation ($SGR > 0$ and $SGR < SGR_{max}$, beige) or to growth at their maximal temperature-, light- and size-dependent growth capacity ($SGR = SGR_{max}$, brown). The composites for Buchan/Banks in September (**a**) and Downs in December (**b**) are shown. Black dashed lines show the length ranges, where the largest yolk-sac larvae were observed and which were used as a proxy for the largest larval length-at-first-feeding (LFF) in this study. Black solid lines show larval LFF calculated after Hufnagl and Peck (2011) and dotted lines depict LFF reported by Blaxter and Hempel (1963).

Simulation 2: Predicted larval growth at the observed feeding conditions

Predicted growth rates of herring larvae differed between the spawning areas and seasons. In both seasons, the proportion of starving larvae decreased with increasing larval size but this decrease was faster in September (Fig. 6a) than in December (Fig. 6b). For example, herring larvae smaller than 8 mm were predicted to starve at more than 74% of the

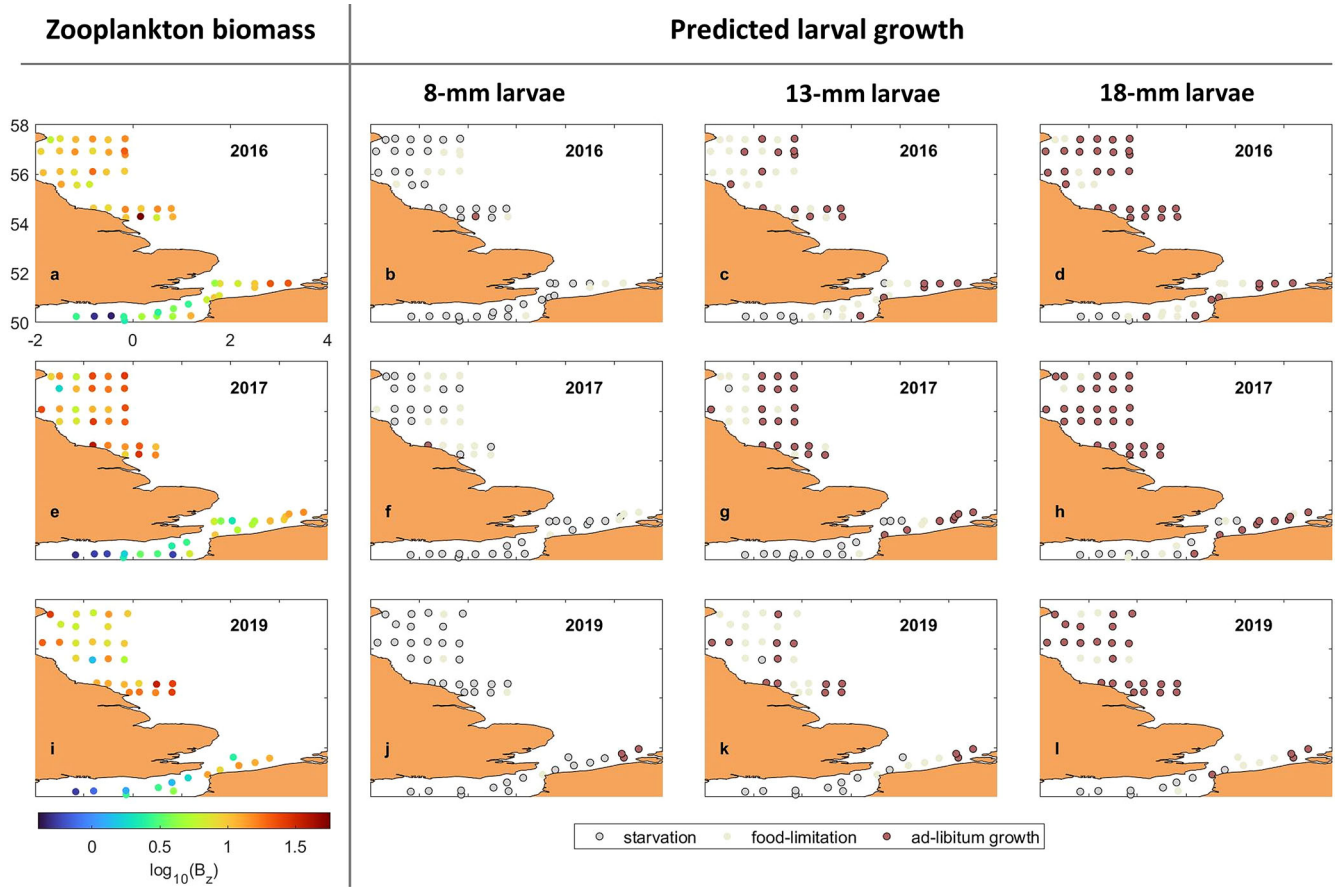

Fig. 7. The observed plankton biomass (B_z, mg m^{-3}) in 2016 (**a**), 2017 (**e**) and 2019 (**i**) and corresponding larval growth predicted for 8-mm (**b**, **f**, **j**), 13-mm (**c**, **g**, **k**) and 18-mm herring larvae (**d**, **h**, **l**). Color coding resembles one of Fig. 6. Please find the corresponding figure for the years 2013, 2014 and 2018 in the supplemental materials (Fig. S5).

stations in the Buchan/Banks area, whereas this percentage decreased to 5%–10% for the bigger first feeding larvae of 9.7–10.8 mm, observed in the survey (dashed lines in Fig. 6a). The proportion of stations supporting "ad-libitum" larval growth increased over 50% for larvae larger than 15 mm and the vast majority of 18-mm larvae were well-fed. In Downs, over 60% of the stations did not provide enough food to support survival of potentially first feeding larvae smaller than 11.9–13.0 mm, which was the maximal larval LFF observed in the December survey (dashed lines in Fig. 6b). Even larvae larger than 18 mm experienced starvation at more than 35% of the stations. The proportion of stations supporting an "ad-libitum" growth of herring larvae increased with the larval size but remained below 40% of all stations sampled in Downs during winter (Fig. 6b).

To depict the spatial pattern in predicted larval growth we used 3 years with the full plankton data coverage (2016, 2017, and 2019). Other years are shown in supplementary materials (S5 "The modelled larval growth in 2013, 2014, and 2018"). The observed prey biomass in all 3 years had a similar spatial pattern with the highest prey biomass in the northern North Sea (in Buchan/Banks areas) and the lowest prey concentration in the English Channel in winter (Fig. 7a,e,i). The zooplankton biomass observed in the Southern Bight in December was comparable with that in the Buchan/Banks areas in September. In all sampled years, prey biomass had a patchy structure with up to 10-fold differences in biomass between neighboring stations. This patchiness was reflected in the spatial distribution of predicted larval growth, which was particularly obvious for the smaller herring larvae. In agreement with Fig. 6, only 26% of all stations supported growth and survival of 8-mm larvae and those stations were broadly distributed across the sampling area (Fig. 7b,f,j). Larger larvae, as it is shown using an example of 13 mm (Fig. 7c,g,k) and 18 mm (d, h, and l) larvae, found enough food to grow at almost all observed stations, except those in the English Channel. The low zooplankton biomass (< 2 mg m^{-3}) observed there caused a strong food deprivation of herring larvae of all tested sizes.

Simulation 3: Optimal and future feeding conditions

The minimal zooplankton biomass B_{min} required by a herring larva to sustain its growth varied with larval size and with the slope of the zooplankton size-spectrum (Fig. 8). As we can see from the example of an 8-mm larva (Fig. 8a,d), B_{min} reached its absolute minimum at a slope of -0.93 (considered to be "optimal") and was higher at the steeper and shallower slopes. Similar patterns of B_{min} were obtained for larger herring larvae (*see* Fig. 8b,c,e,f), although an asymmetric distribution was observed with increasing larval size, that is, a higher

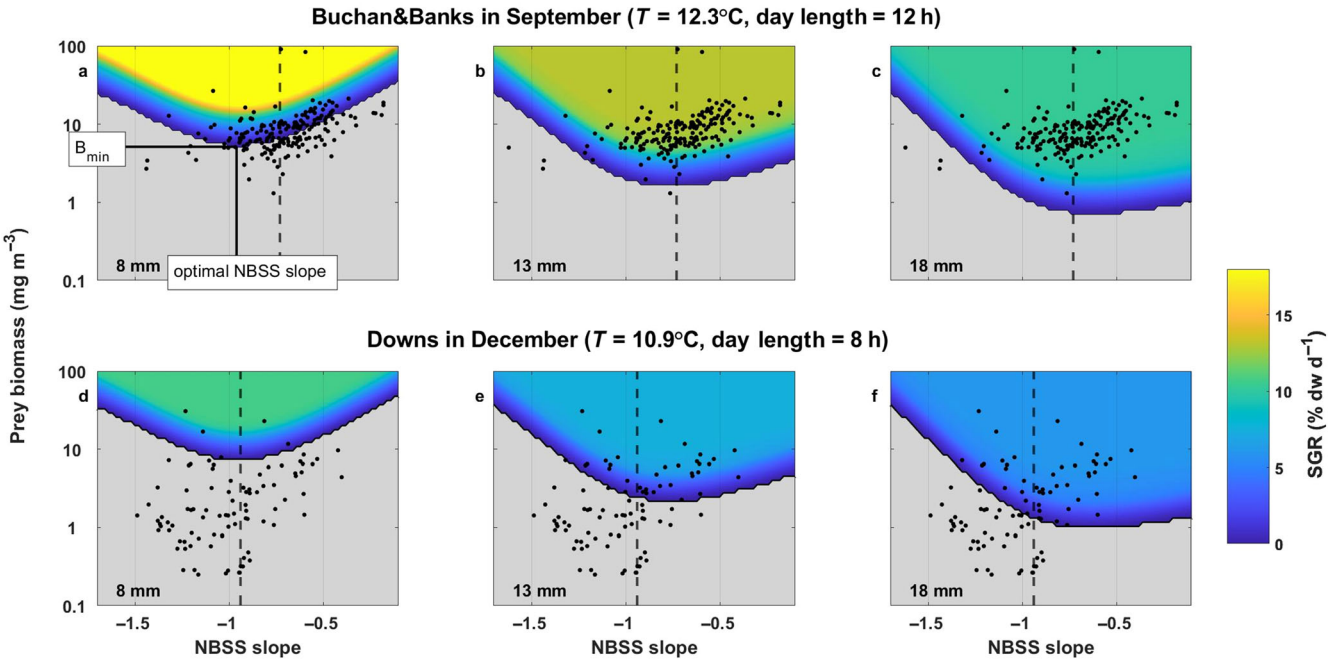

Fig. 8. Modeled growth rate of herring larvae of 8 mm (**a** and **d**), 13 mm (**b** and **e**) and 18 mm (**c** and **f**) length foraging at various prey conditions (prey biomass and NBSS slope) in Buchan/Banks in September (a–c) and in Downs in December (d–f). Colors identify simulated specific growth rates (SGR in % dw d^{-1}), gray color marks the area where the predicted growth rate was negative (SGR < 0), that is, the larvae starved. The minimal biomass B_{min} required by a larva to sustain its growth and the corresponding optimal NBSS slope are marked in the panel a. Larval growth was modeled at the mean observed temperature and light conditions in corresponding spawning areas (Buchan/Banks: $T = 12.3$°C, photoperiod = 12 h; Downs: $T = 10.9$°C, photoperiod = 8 h). Black dots depict the observed prey fields (NBSS slope and biomass) in all sampled years and stations within corresponding spawning areas. Dashed vertical lines identify the median observed NBSS slope.

biomass was required at steeper slopes (those approaching −1.7) than at shallower ones (approaching −0.1). In September, the median observed slope was shallower than the optimal NBSS slope for an 8-mm larva (Fig. 8a), but close to the optimal slope predicted for larger larvae (Fig. 8b,c). In contrast, the median observed NBSS slope in December was close to the optimal slope for smaller 8-mm larvae but steeper than the optimal slope predicted for the larger larvae (Fig. 8d–f). In agreement with Fig. 6, a larger proportion of stations provided insufficient prey (the observed biomass below B_{min}) to support larval growth in Downs in December (Fig. 8d–f) compared to Buchan/Banks in September (Fig. 8a–c).

The optimal NBSS slope was found to increase with larval length from −1.0 to −0.7 for 5-mm to 27-mm larvae (Fig. 9a) and was within the observed range of the NBSS slope. The B_{min} exponentially decreased with the larval length (Fig. 9b): the smallest (5 mm) larvae required at least 67 mg m^{-3} to sustain their growth, whereas larger larvae (e.g., 20 mm) required

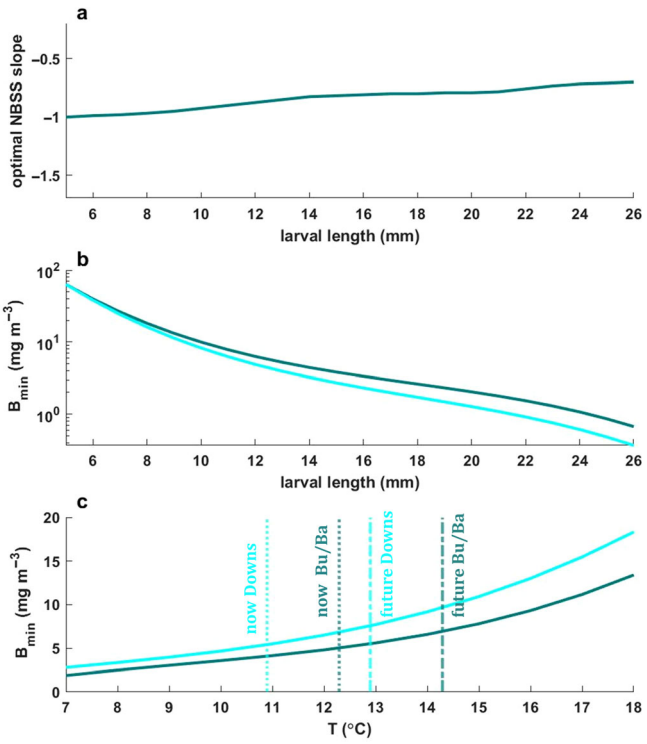

Fig. 9. (**a**) Optimal NBSS slope in September as a function of the initial larval length (optimal NBSS slope in December was identical). (**b**) Minimal required biomass B_{min} obtained with the mean environmental conditions in September (teal, $T = 12.3$°C, photoperiod = 12 h) and December (cyan, $T = 10.9$°C, photoperiod = 8 h). Please note the log-scale along the y-axis. (**c**) Minimal required biomass B_{min} predicted for a 13-mm herring larva in the model simulations with the photoperiod of 12 h (teal, September), and 8 h (cyan, December) but with water temperature varying between 9°C and 16°C. The vertical lines depict current (dotted) and projected (dashed) mean temperatures in the Buchan/Banks (teal) and the Downs (cyan) areas.

10-fold lower prey biomass (1.66 mg m^{-3}). On average, B_{min} was 19% higher in December than in September due to a shorter photoperiod in winter compared to autumn. Furthermore, B_{min} was predicted to increase with temperature in both areas (Fig. 9c), but the rate of increase was slightly different due to different photoperiod and, thus, a duration of the active feeding in autumn and winter. Given a projected 2°C increase of the mean water temperature in the North Sea by the end of the 21st century, our model predicted that B_{min} for a 13-mm larva would increase from 5.6 to 7.6 mg m^{-3} (+35%) in the Downs and from 5.0 to 6.4 mg m^{-3} (+28%) in the Buchan/Banks.

Discussion

To improve our understanding of biotic and abiotic factors affecting marine fish recruitment, there is a need to better resolve processes impacting larval growth and mortality, which is challenging in marine ecosystems (Pepin et al. 2015; Hinchliffe et al. 2021). Here, we addressed two major gaps in knowledge regarding feeding and growth of larval fish: (1) the difference in energetic needs between a specialist vs generalist feeding strategy, and (2) the food-limited growth and starvation during periods of low secondary productivity (e.g., wintertime in temperate ecosystems). The approach taken here of combining simultaneous sampling of fish larvae and their planktonic prey with physiological modeling seems to be a plausible method to explore larval growth and its variability particularly in a food-limited environment. We argue that covering a wide size-range of potential prey is necessary to properly assess feeding conditions experienced by fish larvae. Using automated identification and size measuring would be a recommended approach as it is substantially less time-consuming compared to classical microscopy (Orenstein et al. 2022) but still provides sufficient information to accurately estimate larval growth by means of bioenergetic modeling. It is well suited to expand the existing larval monitoring programs providing estimates of larval abundance for the routine stock assessments toward more holistic ecosystem surveys.

Feeding modes of herring larvae and the role of microplankton

Previously reported field-based estimates of prey preference of herring larvae agree poorly. Some studies reported a clear preference of larvae for copepods, with a shift from smaller to larger stages or species of copepods with increasing larval size (e.g., Kiørboe et al. 1988; Wilson et al. 2018). More recent studies suggested that young herring larvae are generalist foragers, ingesting a wider range of proto- and microplankton organisms (de Figueiredo et al. 2005; Bils et al. 2016; Denis et al. 2016). Our feeding scenarios provided some insight on a likely feeding strategy of larvae from the bioenergetic perspective.

Our results suggest that "specialist" feeders (only copepods) needed to be, on average, 2-mm larger on the onset of the

exogeneous feeding than "generalist" feeders to sustain positive growth and survive (Fig. 4). Moreover, growth rates of young herring larvae were, on average, 40% lower in the "specialist" compared to the "generalist" scenario. Similar estimates of reduced growth were obtained by Bils et al. (2016). Such difference in growth may result in substantial reductions in larval survival since mortality rates are believed to decrease rapidly with increasing larval size (Houde 2002). Payne et al. (2013) estimated that a 10% reduction in growth can result in a 60–80% reduction in the number of herring larvae surviving to metamorphosis. Our results suggest that focusing only on copepods as a prey item of herring larvae (as Kühn et al. 2008, Alvarez-Fernandez et al. 2015, or Hufnagl et al. 2015) could potentially lead to an underestimation of larval growth and survival, particularly when early-feeding herring larvae are of concern.

A higher survival potential and faster growth of herring larvae in the generalist scenario was mainly due to the broader range of microplankton prey species included in the larval diet. According to our observations, copepods formed on average only 20% of the observed biomass of microplankton (20 to 200 μm) suitable for larval foraging (Fig. S4), other 80% mainly consisted of diatoms, bivalve larvae, foraminiferans, and ciliates. Our estimate of 38% of microplankton in the diet of an 8-mm larva was well within 19–71% proportion of microplankton prey in the diet of herring larvae reported by de Figueiredo et al. (2005). Larger herring larvae were predicted to be able to reach their maximal growth capacity by feeding only on copepods (Fig. 4). This was in agreement with Denis et al. (2016) who showed that protists constituted a relevant part of the diet of Downs herring larvae smaller than 12 mm, whereas bigger larvae were selective toward copepods and dinoflagellates. We need to keep in mind, however, that field studies of larval diet are generally associated with challenges including the identification of small, rapidly digested planktonic prey (e.g., naked dinoflagellates, appendicularians or other microplankton) in the gut of a fish larva (Llopiz et al. 2010; Denis et al. 2016; Suthers et al. 2022). The consumption rates reported for those prey organisms in field-caught larvae are probably often underestimated, as suggested in de Figueiredo et al. (2005).

Observed feeding conditions and modeled larval growth

According to the 7 years of observations used in this study, different feeding conditions (i.e., temperature, photoperiod, zooplankton biomass) in Buchan/Banks and Downs areas yielded different growth and survival potential of herring larvae (Fig. 6). Even in the most favorable "generalist" feeding scenario, food limitation was an important factor affecting small larvae in both areas. Larger larvae (> 18 mm) were predicted to experience food-limitation in winter at Downs, but not in autumn at Buchan/Banks, where larvae approached their maximal temperature- and size-specific growth capacity at the vast majority of the stations. These results agree well with Kiørboe et al. (1988) and Buckley and Durbin (2006) who showed a strong prey-limitation of young larvae, but not of larger larvae captured at the same station.

Our findings for the Buchan/Banks areas are in line with the "critical period" hypothesis, which postulates an exceptionally high starvation mortality of first-feeding fish larvae in marine ecosystems (Hjort 1914). Alvarez-Fernandez et al. (2015) and Fässler et al. (2011) supported the importance of the first-feeding period for the recruitment success of herring in the North Sea. In contrast to the autumn larvae, the winter larvae in the Downs area in our study had a substantial probability of starvation over a wider range of larval lengths and, therefore, well beyond the first-feeding period (Fig. 6). This suggests that survival of winter herring larvae is not driven by a short "critical" event but by continual losses due to starvation over the protracted overwintering period in agreement with Hufnagl et al. (2015). Our findings, however, showed that only the English Channel was characterized by low zooplankton concentrations and, thus, a high proportion of starving larvae over the observed period, whereas the zooplankton availability in the Southern Bight was rather similar to those in Buchan/Banks (Fig. 7). Given the prevailing direction of water currents (Fig. 1) in this area, herring larvae hatched in the English Channel are gradually transported to the Southern Bight (Hufnagl et al. 2015) where, according to our results, they would find more favorable feeding conditions. However, herring larvae of all size classes between 5 and 24 mm were observed in the English Channel and those larvae were probably strongly affected by starvation.

A higher probability of starvation predicted for Downs compared to Buchan/Banks larvae is difficult to reconcile with the increasing relative contribution of Downs larvae to the overall NSASH recruitment in the most recent years (ICES 2022). One possible explanation is that the increased risk of larval starvation is counterbalanced by a decreased risk of predation mortality of young herring larvae during winter. Indeed, Pepin (1991) and Akimova et al. (2016) suggested a reduced predation pressure on fish early-life stages during winter due to a decrease in activity, appetite and feeding rate of predators at cold temperatures. Another possible explanation could be a recent decrease in the relative proportion of Buchan/Banks larvae due to a decline in their survival. Our simulations predicted a rapid decrease in the probability of starvation with increasing larval size, suggesting that larger first-feeding larvae have a substantially better chance of surviving (finding enough food to support their growth) in this area compared to their smaller siblings. The observed temperature increase in the Buchan/Banks area during the last decade (e.g., Fässler et al. 2011) could potentially cause a decrease of the LFF of herring larvae (Geffen 2009; van Damme et al. 2009; Peck et al. 2012) and, thereby, augment larval susceptible to starvation. Our results underscore the need for up-to-date and quality-assured estimates of the hatch and first-feeding lengths of herring larvae from different spawning

components in the North Sea (and probably, elsewhere) in order to accurately estimate larval starvation mortality. Novel, mobile mesocosm experimental setup with underwater video recordings (e.g., Sswat et al. 2018) could help to overcome the problem that herring larvae often lose their yolk-sac if handled.

Optimal and future foraging of herring larvae

The modeled growth rate of herring larvae was sensitive to both plankton biomass and size structure (NBSS slope). The sensitivity of young herring larvae to changes in the NBSS slope (Fig. 8) was due to the fact that the proportion of zooplankton biomass within a suitable size-range available for larval foraging depended on the NBSS slope. If the slope was too shallow (less steep than the optimal) the number of prey smaller than the larval gape opening was insufficient to support larval growth. If the slope was too steep, there was too few larger energy-rich prey organisms available for larvae. Herring larvae were predicted to become less sensitive to the less negative slopes (more larger prey items) as they grow, because larger larvae become more efficient in utilizing larger prey organisms (Fig. 8). This also explains why the optimal NBSS slope becomes less negative as the larval size increased (Fig. 9a). The importance of the zooplankton size structure for larval growth has been previously emphasized by Urtizberea and Fiksen (2013), David et al. (2022) and Huebert and Peck (2014), although the results of the latter were somewhat different from ours (*see* more details in the supplementary materials S6 "Model sensitivity to NBSS slope"). Furthermore, Suthers et al. (2022) hypothesized a key role of the slope of the zooplankton size spectra in shaping growth and survival of fish larvae in marine ecosystems. Such dependency of larval growth and survival on zooplankton size structure could potentially provide a new context in quantifying or predicting fish recruitment.

The minimal biomass of micro- and mesozooplankton in the size range between 20 and 2000 μm required to support larval growth was shown to decrease with the larval size, despite of the fact that bigger larvae require a higher absolute amount of consumed food to grow. This can be explained by a limited ability of small larvae to utilize their prey field due to their limited motility. A more detailed explanations is provided in the supplementary materials (S7 "Minimal prey biomass required for a positive larval growth"). Furthermore, our bioenergetic model predicted that the minimal prey biomass required for larval growth was, on average, 19% higher in December than in September (Fig. 9b). The reason for the higher prey requirements in winter, despite colder temperatures, was the relatively short photoperiod and, thus, longer period of time when larvae do not gain energy from prey but continue to pay for metabolic costs. The energy savings afforded by colder temperatures in December does not fully compensate for the increased loss of foraging time at the relatively short, wintertime photoperiods. Projected warming will increase energetic costs and, therefore, be particularly challenging for larvae experiencing short photoperiods. We estimated that a 13-mm herring larva will require 28% (35%) higher prey biomass in the Buchan/Banks (Downs) area to sustain their growth in the 2°C-warmer North Sea. It remains an open question whether the productivity of the North Sea will increase in the future, or Atlantic herring will adapt its spawning strategy, including phenology and/or distributional shift, to promote larval survival as it is known for various marine fish species (e.g., Bakun 2006; Ottmann et al. 2021). Long-term climate variability have caused past shifts in the spawning season of herring in different ecosystems (ICES 2005; Moyano et al. 2023) and the ongoing global warming could potentially drive the shifts in phenology (or prey requirements) beyond tolerable thresholds for the persistence of some populations in the future. Therefore, feeding processes and adaptation strategies are of great interest in species with considerable plasticity such as Atlantic herring.

Uncertainties and critical knowledge gaps

Limitations of the bioenergetic model

Although the model used in this study yielded a good comparison with larval growth reported by previous laboratory and field studies (Hufnagl and Peck 2011; Bils et al. 2016; Illing et al. 2018), there are some important limitations to our modeling approach. First, zooplankton traits relevant for larval foraging (i.e., those impacting a larva's visual detection, capture success and handling time of prey) were considered solely size-dependent and not impacted by prey species (S3 "Model description"). Size is likely an important factor in larval prey selectivity and the modeled foraging niche compares well with the observed one (Hufnagl and Peck 2011), nonetheless, this assumption probably oversimplifies the complexity of prey–predator relationships in marine larvae. A number of previous studies have shown that fish larvae consistently select certain zooplankton species over others, probably because of their lower motility, shorter handling time (including pursue, capture and digestion) or better visibility (i.e., pigmentation) in comparison to other species of the same size (*see* review papers of Nunn et al. 2012, Litchman et al. 2013, and Robert et al. 2014). Such species-specific traits, as far as are known, can be incorporated in a mechanistic foraging model as one used by Petrik et al. (2009) and can potentially alter predicted larval growth depending on the relative abundance of the preferred prey of herring larvae. In our opinion, further field foraging studies combining multiple approaches (such as visual gut content analysis, DNA metabarcoding and isotope analysis) will be required to validate such models and to better understand dietary preferences of herring larvae at various feeding conditions.

Second, the metabolic rates used in this study were temperature- and size-dependent (*see* S3 "Model description"), and did not consider metabolic down-regulation of herring larvae at poor feeding conditions. Kiørboe et al. (1987) and

Illing et al. (2018) reported the metabolic rates of a starving larva being 8–34% lower than those of a well-fed one. Such energy-saving mechanism is probably linked to the starvation resistance of herring larvae that allow them to survive at zero-growth rates in laboratory experiments whereas larvae of other species such as cod need to maintain a positive growth (e.g., 3% d^{-1}) to survive (Folkvord et al. 2015). However, the positive effects of such metabolic down-regulation on larval survival remain questionable. Low or zero-growth increases a size-dependent predation pressure on larvae in agreement with the "bigger is better" and "stage duration" hypotheses (Anderson 1988; Houde 2008). A better understanding of a decreased performance of starved larvae and larval resilience to unfavorable feeding conditions (e.g., duration to point-of-no-return of yolk-sac and pre-flexion larvae) will be required to estimate larval mortality in different seasons.

Prey field

Although we applied a novel sampling strategy that simultaneously captured larval fish and a broad range of planktonic prey sizes, there are several limitations to our approach. First, some microplankton organisms in the 20–55 μm range were missing in the samples due to the mesh size of 55 μm and some soft-bodied microplankton organisms were lost due to the preservation in formalin (*see* S1 "Plankton data"). This can potentially cause a positive bias of the slope (shallower slopes) of the NBSS built on those data and an underestimation of the prey biomass available for larval feeding and growth. We expect this to be particularly important for the smaller, potential first-feeding larvae that were predicted to be more susceptible to starvation in both spawning areas/seasons.

Moreover, one needs to be aware that our net sampling represents an "average" prey concentration across $\sim$ 2 km tow distance at each station. Despite finding substantial variability in the distribution of zooplankton biomass between sampled stations (Fig. 7), our data provide no information about a small-scale (10s of meter) plankton patchiness that has been suggested to enhance growth rates and sustain survival of larval fish experiencing suboptimal feeding conditions (e.g., Davis et al. 1991; Pitchford and Brindley 2001; Pepin et al. 2015). Alternative observational methods, for example, a Video Plankton Recorder (Davis et al. 2005; Lough and Broughton 2006) or similar equipment could be used in the future to resolve the fine-scale patchiness in the distribution of fish larvae and their prey. This information is particularly valuable for the food-limited environments such as the winter North Sea.

Our modeling approach did not consider the impact of larval feeding on zooplankton and the ability of herring larvae to overgraze its zooplankton prey. Pepin and Penney (2000) and Llopiz et al. (2010) found it rather unlikely that the foraging of larval fish can significantly reduce zooplankton standing stocks, whereas Cushing (1983) and Maar et al. (2014) suggested the opposite. Although larval prey consumption will likely have little impact if foraging occurs in a patch of high zooplankton biomass, intraguild competition and overgrazing may increase the risk of larval starvation when prey availability or productivity is low. To our knowledge, such feedback has been largely ignored in individual-based bioenergetic models of marine fish larvae. To add more realism to larval foraging models, such density-dependent effects and feedback loops on the prey field need to be considered in future studies.

Data Availability Statement

Herring larvae and hydrographic data are available from the ICES data portals (https://www.ices.dk/data/data-portals/Pages/Eggs-and-larvae.aspx) and (https://www.ices.dk/data/data-portals/Pages/ocean.aspx), respectively. Zooplankton data are available via Figshare Data portal (https://doi.org/10.6084/m9.figshare.23506629.v1).

References

Akimova, A., I. Núñez-Riboni, A. Kempf, and M. H. Taylor. 2016. Spatially-resolved influence of temperature and salinity on Stock and recruitment variability of commercially important fishes in the North Sea. PLoS One **11**: e0161917. doi:10.1371/journal.pone.0161917

Álvarez, E., M. Moyano, Á. López-Urrutia, E. Nogueira, and R. Scharek. 2013. Routine determination of plankton community composition and size structure: A comparison between FlowCAM and light microscopy. J. Plankton Res. **36**: 170–184. doi:10.1093/plankt/fbt069

Alvarez-Fernandez, S., P. Licandro, C. J. G. van Damme, and M. Hufnagl. 2015. Effect of zooplankton on fish larval abundance and distribution: A long-term study on North Sea herring (*Clupea harengus*). ICES J. Mar. Sci. **72**: 2569–2577. doi:10.1093/icesjms/fsv140

Anderson, J. T. 1988. A review of size dependent survival during prerecruit stages of fishes in relation to recruitment. J. Northwest Atl. Fish. Sci. **8**: 55–56. doi:10.2960/J.v8.a6

Bailey, K. M., and E. D. Houde. 1989. Predation on eggs and larvae of marine fishes and the recruitment problem. Adv. Mar. Biol. **25**: 1–83. doi:10.1016/S0065-2881(08)60187-X

Bakun, A. 2006. Wasp-waist populations and marine ecosystem dynamics: Navigating the "predator pit" topographies. Prog. Oceanogr. **68**: 271–288. doi:10.1016/j.pocean.2006.02.004

Bils, F., M. Moyano, N. Aberle, M. Hufnagl, S. Alvarez-Fernandez, and M. A. Peck. 2016. Exploring the microzooplankton–ichthyoplankton link: A combined field and modeling study of Atlantic herring (*Clupea harengus*) in the Irish Sea. J. Plankton Res. **39**: 147–163. doi:10.1093/plankt/fbw074

Blanco, J. M., F. Echevarría, and C. García. 1994. Dealing with size-spectra: Some conceptual and mathematical problems. Sci. Mar. **58**(1-2): 17–29.

Blaxter, J. H. S., and G. Hempel. 1963. The influence of egg size on herring larvae (*Clupea harengus* L.). ICES Mar. Sci. **28**(2): 211–240. doi:10.1093/icesjms/28.2.211

Buckley, L. J., and E. G. Durbin. 2006. Seasonal and interannual trends in the zooplankton prey and growth rate of Atlantic cod (*Gadus morhua*) and haddock (*Melanogrammus aeglefinus*) larvae on Georges Bank. Deep-Sea Res. II Top. Stud. Oceanogr. **53**: 2758–2770. doi:10.1016/j.dsr2.2006.08.009

Chambers, R. C., and E. A. Trippel [eds.]. 1997. Early life history and recruitment in fish populations. *In* Fish and fisheries series. Chapman & Hall. doi:10.1073/pnas.94.4.1258

Cushing, D. H. 1983. Are fish larvae too dilute to affect the density of their food organisms? J. Plankton Res. **5**: 847–854. doi:10.1093/plankt/5.6.847

Cushing, D. H. 1990. Plankton production and year-class strength in fish populations: An update of the match/mismatch hypothesis, p. 249–293. *In* J. H. S. Blaxter and A. J. Southward [eds.], Advances in marine biology, v. **26**. Academic Press. doi:10.1016/S0065-2881(08)60202-3

van Damme, C., M. Dickey-Collas, A. Rijnsdorp, and O. Kjesbu. 2009. Fecundity, atresia, and spawning strategies of Atlantic herring (*Clupea harengus*). Can. J. Fish. Aquat. Sci. **66**: 2130–2141. doi:10.1139/F09-153

David, C. L., R. Ji, C. Bouchard, H. Hop, and J. A. Hutchings. 2022. The interactive effects of temperature and food consumption on growth of larval Arctic cod (*Boreogadus saida*): A bioenergetic model. Elementa Sci. Anthropocene **10**. doi:10.1525/elementa.2021.00045

Davis, C. S., G. R. Flierl, P. H. Wiebe, and P. J. S. Franks. 1991. Micropatchiness, turbulence and recruitment in plankton. J. Mar. Res. **49**: 109–151. doi:10.1357/002224091784968602

Davis, C. S., F. T. Thwaites, S. M. Gallager, and Q. Hu. 2005. A three-axis fast-tow digital video plankton recorder for rapid surveys of plankton taxa and hydrography. Limnol. Oceanogr.: Methods **3**: 59–74. doi:10.4319/lom.2005.3.59

Denis, J., C. Vallet, L. Courcot, V. Lefebvre, J. Caboche, E. Antajan, P. Marchal, and C. Loots. 2016. Feeding strategy of downs herring larvae (*Clupea harengus* L.) in the English Channel and North Sea. J. Sea Res. **115**: 33–46. doi:10.1016/j.seares.2016.07.003

Dickey-Collas, M., and others. 2010. Lessons learned from stock collapse and recovery of North Sea herring: A review. ICES J. Mar. Sci. J. Conseil **67**: 1875–1886. doi:10.1093/icesjms/fsq033

Fässler, S., M. Payne, T. Brunel, and M. Dickey-Collas. 2011. Does larval mortality influence population dynamics? An analysis of North Sea herring (*Clupea harengus*) time series. Fish. Oceanogr. **20**: 530–543. doi:10.1111/j.1365-2419.2011.00600.x

de Figueiredo, G. M., R. D. M. Nash, and D. J. S. Montagnes. 2005. The role of the generally unrecognised microprey source as food for larval fish in the Irish sea. Mar. Biol. **148**: 395–404. doi:10.1007/s00227-005-0088-0

Folkvord, A., K. W. Vollset, and I. A. Catalán. 2015. Differences in growth and survival between cod *Gadus morhua* and herring *Clupea harengus* early stages co-reared at variable prey concentrations. Comp. Study **87**: 1176–1190. doi:10.1111/jfb.12783

Fuiman, L. A., and R. G. e. Werner. 2002. Fishery science: The unique contributions of early life stages. Blackwell Science Ltd. ISBN: 978-0-632-05661-3.

Geffen, A. J. 2009. Advances in herring biology: From simple to complex, coping with plasticity and adaptability. ICES J. Mar. Sci. **66**: 1688–1695. doi:10.1093/icesjms/fsp028

Hinchliffe, C., P. Pepin, I. M. Suthers, and D. S. Falster. 2021. A novel approach for estimating growth and mortality of fish larvae. ICES J. Mar. Sci. **78**: 2684–2699. doi:10.1093/icesjms/fsab161

Hjort, J. 1914. Fluctuations in the great fisheries of northern Europe. Rapp. P-V Réun. **20**: 1–228.

Houde, E. D. 2002, p. 64–87. *In* L. A. Fuiman and R. G. Werner [eds.], Mortality. Fishery science. The 268 unique contributions of early life stages. Blackwell Publishing. ISBN: 978-0-632-05661-3.

Houde, E. D. 2008. Emerging from Hjort's shadow. J. Northwest Atl. Fish. Sci. **41**: 53–70. doi:10.2960/J.v41.m634

Huebert, K. B., and M. A. Peck. 2014. A day in the life of fish larvae: Modeling foraging and growth using quirks. PLoS ONE **9**: e98205. doi:10.1371/journal.pone.0098205

Huebert, K. B., J. Pätsch, M. Hufnagl, M. Kreus, and M. A. Peck. 2018. Modeled larval fish prey fields and growth rates help predict recruitment success of cod and anchovy in the North Sea. Mar. Ecol. Prog. Ser. **600**: 111–126. doi:10.3354/meps12615

Hufnagl, M., and M. A. Peck. 2011. Physiological individual-based modelling of larval Atlantic herring (*Clupea harengus*) foraging and growth: Insights on climate-driven life-history scheduling. ICES J. Mar. Sci. **68**: 1170–1188. doi:10.1093/icesjms/fsr078

Hufnagl, M., M. A. Peck, R. D. M. Nash, and M. Dickey-Collas. 2015. Unravelling the gordian knot! Key processes impacting overwintering larval survival and growth: A North Sea herring case study. Prog. Oceanogr. **138**: 486–503. doi:10.1016/j.pocean.2014.04.029

ICES. 2005. Spawning and life history information for North Atlantic cod stocks, p. 152. *In* K. M. E. Brander [ed.], ICES cooperative research report. ICES.

ICES. 2022. Herring assessment working group for the area south of 62° N (HAWG). ICES Sci. Rep. **4**: 745.

Illing, B., M. Moyano, J. Berg, M. Hufnagl, and M. A. Peck. 2018. Behavioral and physiological responses to prey match-mismatch in larval herring. Estuar. Coast. Shelf Sci. **201**: 82–94. doi:10.1016/j.ecss.2016.01.003

Kiørboe, T., P. Munk, and K. Richardson. 1987. Respiration and growth of larval herring *Clupea harengus*: Relation between specific dynamic action and growth efficiency. Mar. Ecol. Prog. Ser. **40**: 1–10. doi:10.3354/meps040001

Kiørboe, T., P. Munk, K. Richardson, V. Christensen, and H. Paulsen. 1988. Plankton dynamics and larval herring growth, drift and survival in a frontal area. Mar. Ecol. Prog. Ser. **44**: 205–219. doi:10.3354/meps044205

Kühn, W., M. A. Peck, H. H. Hinrichsen, U. Daewel, A. Moll, T. Pohlmann, C. Stegert, and S. Tamm. 2008. Defining habitats suitable for larval fish in the German bight (southern North Sea): An IBM approach using spatially- and temporally-resolved, size-structured prey fields. J. Mar. Syst. **74**: 329–342. doi:10.1016/j.jmarsys.2008.02.002

Last, J. M. 1978. The food of four species of pleuronectiform larvae in the eastern English Channel and southern North Sea. Mar. Biol. **45**: 359–368. doi:10.1007/BF00391822

Letcher, B. H., J. A. Rice, L. B. Crowder, and K. A. Rose. 1996. Variability in survival of larval fish: disentangling components with a generalized individual-based model. Can. J. Fish Aqua. Sci. **53**(4): 787–801. doi:10.1139/f95-241

Litchman, E., M. D. Ohman, and T. Kiørboe. 2013. Trait-based approaches to zooplankton communities. J. Plankton Res. **35**: 473–484. doi:10.1093/plankt/fbt019

Llopiz, J. K. 2013. Latitudinal and taxonomic patterns in the feeding ecologies of fish larvae: A literature synthesis. J. Mar. Syst. **109**: 69–77. doi:10.1016/j.jmarsys.2012.05.002

Llopiz, J. K., D. E. Richardson, A. Shiroza, S. L. Smith, and R. K. Cowen. 2010. Distinctions in the diets and distributions of larval tunas and the important role of appendicularians. Limnol. Oceanogr. **55**: 983–996. doi:10.4319/lo.2010.55.3.0983

Lough, R. G., and E. A. Broughton. 2006. Development of microscale frequency distributions of plankton for inclusion in foraging models of larval fish, results from a video plankton recorder. J. Plankton Res. **29**: 7–17. doi:10.1093/plankt/fbl055

Maar, M., A. Rindorf, E. F. Møller, A. Christensen, K. S. Madsen, and M. van Deurs. 2014. Zooplankton mortality in 3D ecosystem modelling considering variable spatial–temporal fish consumptions in the North Sea. Prog. Oceanogr. **124**: 78–91. doi:10.1016/j.pocean.2014.03.002

Moyano, M., and others. 2023. Caught in the middle: Bottom-up and top-down processes impacting recruitment in a small pelagic fish. Rev. Fish Biol. Fish. **33**: 55–84. doi:10.1007/s11160-022-09739-2

Nash, R. D. M., and M. Dickey-Collas. 2005. The influence of life history dynamics and environment on the determination of year class strength in North Sea herring (*Clupea harengus* L.). Fish. Oceanogr. **14**: 279–291. doi:10.1111/j.1365-2419.2005.00336.x

Nash, R. D. M., M. Dickey-Collas, and S. P. Milligan. 1998. Descriptions of the Gulf VH/PRO-NET and MAFF/Guildline unencased high-speed plankton samplers. J. Plankton Res. **20**: 1915–1926. doi:10.1093/plankt/20.10.1915

Nunn, A. D., L. H. Tewson, and I. G. Cowx. 2012. The foraging ecology of larval and juvenile fishes. Rev. Fish Biol. Fish. **22**: 377–408. doi:10.1007/s11160-011-9240-8

Orenstein, E. C., and others. 2022. Machine learning techniques to characterize functional traits of plankton from image data. Limnol. Oceanogr. **67**: 1647–1669. doi:10.1002/lno.12101

Ottmann, D., Ø. Fiksen, M. Martín, F. Alemany, L. Prieto, D. Álvarez-Berastegui, and P. Reglero. 2021. Spawning site distribution of a bluefin tuna reduces jellyfish predation on early life stages. Limnol. Oceanogr. **66**: 3669–3681. doi:10.1002/lno.11908

Payne, M. R., and others. 2009. Recruitment in a changing environment: The 2000s North Sea herring recruitment failure. ICES J. Mar. Sci. J. Conseil **66**: 272–277. doi:10.1093/icesjms/fsn211

Payne, M., S. Ross, L. Worsøe Clausen, P. Munk, H. Mosegaard, and R. D. M. Nash. 2013. Recruitment decline in North Sea herring is accompanied by reduced larval growth rates. Mar. Ecol. Prog. Ser. **489**: 197–211. doi:10.3354/meps10392

Peck, M. A., K. B. Huebert, and J. K. Llopiz. 2012. Intrinsic and extrinsic factors driving match-mismatch dynamics during the early life history of marine fishes. Adv. Ecol. Res. **47**: 177–302. doi:10.1016/B978-0-12-398315-2.00003-X

Pepin, P. 1991. Effect of temperature and size on development, mortality, and survival rates of the pelagic early life history stages of marine fish. Can. J. Fish. Aquat. Sci. **48**: 503–518. doi:10.1139/f91-065

Pepin, P., and R. W. Penney. 1997. Patterns of prey size and taxonomic composition in larval fish: Are there general size-dependent models? J. Fish Biol. **51**: 84–100. doi:10.1111/j.1095-8649.1997.tb06094.x

Pepin, P., and R. Penney. 2000. Feeding by a larval fish community: Impact on zooplankton. Mar. Ecol. Prog. Ser. **204**: 199–212. doi:10.3354/meps204199

Pepin, P., and others. 2015. Once upon a larva: Revisiting the relationship between feeding success and growth in fish larvae. ICES J. Mar. Sci. **72**: 359–373. doi:10.1093/icesjms/fsu201

Petrik, C. M., T. Kristiansen, R. G. Lough, and C. S. Davis. 2009. Prey selection by larval haddock and cod on copepods with species-specific behavior: An individual-based model analysis. Mar. Ecol. Prog. Ser. **396**: 123–143. doi:10.3354/meps08268

Pitchford, W. J., and J. Brindley. 2001. Prey patchiness, predator survival and fish recruitment. Bull. Math. Biol. **63**: 527–546. doi:10.1006/bulm.2001.0230

Robert, D., H. M. Murphy, G. P. Jenkins, and L. Fortier. 2014. Poor taxonomical knowledge of larval fish prey preference is impeding our ability to assess the existence of a "critical period" driving year-class strength. ICES J. Mar. Sci. J. Conseil **71**: 2042–2052. doi:10.1093/icesjms/fst198

Schmidt, J., C. van Damme, C. Röckmann, and M. Dickey-Collas. 2009. Recolonisation of spawning grounds in a recovering fish stock: Recent changes in North Sea herring.

Scientia Marina **73**: 153–157. doi:10.3989/scimar.2009.73s1153

Schrum, C., and others. 2016. Projected change—North Sea, p. 175–217. *In* M. Quante and F. Colijn [eds.], North Sea region climate change assessment. Springer International Publishing. doi:10.1007/978-3-319-39745-0

Sheldon, R. W., A. Prakash, and W. H. Sutcliffe Jr. 1972. The size distribution of particles in the ocean. Limnol. Oceanogr. **17**: 327–340. doi:10.4319/lo.1972.17.3.0327

Sswat, M., M. H. Stiasny, J. Taucher, M. Algueró-Muñiz, L. T. Bach, F. Jutfelt, U. Riebesell, and C. Clemmesen. 2018. Food web changes under ocean acidification promote herring larvae survival. Nat. Ecol. Evol. **2**: 836–840. doi:10.1038/s41559-018-0514-6

Suthers, I. M., Z. White, C. Hinchliffe, D. S. Falster, A. J. Richardson, and J. D. Everett. 2022. The mortality/growth ratio of larval fish and the slope of the zooplankton size-spectrum. Fish Fish. **23**: 750–757. doi:10.1111/faf.12633

Urtizberea, A., and Ø. Fiksen. 2013. Effects of prey size structure and turbulence on feeding and growth of anchovy larvae. Environ. Biol. Fishes **96**: 1045–1063. doi:10.1007/s10641-012-0102-6

Wilson, C. J., H. M. Murphy, C. Bourne, P. Pepin, and D. Robert. 2018. Feeding ecology of autumn-spawned Atlantic herring (*Clupea harengus*) larvae in Trinity Bay, Newfoundland: Is recruitment linked to main prey availability? J. Plankton Res. **40**: 255–268. doi:10.1093/plankt/fby003

Acknowledgments

This work has been partially funded by the German Research Foundation (THRESHOLDS, MO 867 2873/3-1) and by the German Federal Ministry of Education and Research (DAM-CoastalFutures, grant 03F0911F). We would like to thank Eva Alvarez, Henrike Andresen and Heino Fock for their help with zooplankton related issues, Björn Illing, Richard Nash and Audrey Geffen for their consulting on larval herring, Klaus Huebert and Marc Hufnagl for providing their model code, Ismael Nunez-Riboni, Tahereh Nakisa and Patrick Polte for valuable discussions, and Andriy Martynenko for his support in data processing. Furthermore, we would like thank two anonymous reviewers and the academic editors, K. David Hambright and James Leichter, for their helpful and constructive comments. Open Access funding enabled and organized by Projekt DEAL.

Conflict of Interest

The authors have no conflicts of interest to declare.

Submitted 04 December 2022
Revised 30 March 2023
Accepted 03 June 2023

Associate editor: James J. Leichter